Journal of Neuroscience Methods 326 (2019) 108357

Contents lists available at ScienceDirect

Journal of Neuroscience Methods

journal homepage: www.elsevier.com/locate/jneumeth

Advances in the automation of whole-cell patch clamp technology

Ho-Jun Suk[a,b,c], Edward S. Boyden[b,c,d,e], Ingrid van Welie[f,*]

[a] Health Sciences and Technology, MIT, Cambridge, MA 02139, USA
[b] Media Lab, MIT, Cambridge, MA 02139, USA
[c] McGovern Institute, MIT, Cambridge, MA 02139, USA
[d] Department of Biological Engineering, MIT, Cambridge, MA 02139, USA
[e] Department of Brain and Cognitive Sciences, MIT, Cambridge, MA 02139, USA
[f] Neural Dynamics Technologies LLC, Cambridge, MA 02142, USA

GRAPHICAL ABSTRACT

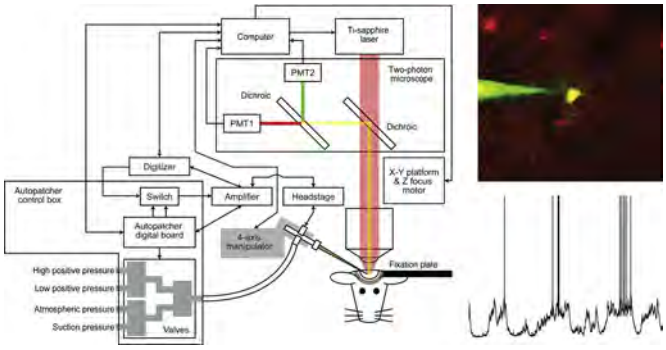

ARTICLE INFO

Keywords:
Electrophysiology
Patch clamp
Automation

ABSTRACT

Electrophysiology is the study of neural activity in the form of local field potentials, current flow through ion channels, calcium spikes, back propagating action potentials and somatic action potentials, all measurable on a millisecond timescale. Despite great progress in imaging technologies and sensor proteins, none of the currently available tools allow imaging of neural activity on a millisecond timescale and beyond the first few hundreds of microns inside the brain. The patch clamp technique has been an invaluable tool since its inception several decades ago and has generated a wealth of knowledge about the nature of voltage- and ligand-gated ion channels, sub-threshold and supra-threshold activity, and characteristics of action potentials related to higher order functions. Many techniques that evolve to be standardized tools in the biological sciences go through a period of transformation in which they become, at least to some degree, automated, in order to improve reproducibility, throughput and standardization. The patch clamp technique is currently undergoing this transition, and in this review, we will discuss various aspects of this transition, covering advances in automated patch clamp technology both *in vitro* and *in vivo*.

* Corresponding author.
E-mail address: ingrid@neuraldynamicstechnologies.com (I. van Welie).

https://doi.org/10.1016/j.jneumeth.2019.108357
Received 2 April 2019; Received in revised form 5 July 2019; Accepted 10 July 2019
Available online 20 July 2019

1. Introduction

The computations performed by the mammalian brain and their information content are transmitted in the form of ionic currents through membrane channels. The patch clamp technique, the gold-standard for electrophysiological characterization of individual neurons, utilizes a glass electrode to achieve electrical access to the inside of the neuronal membrane, enabling low-noise, high-temporal resolution recordings and manipulation of a neuron's electrical signals. Recent advancements in sensor proteins, actuator proteins, and optical tools have enabled "all-optical" approaches to electrophysiology, which utilize fluorescent voltage sensors (Adam et al., 2019; Piatkevich et al., 2019; Hochbaum et al., 2014; Kiskinis et al., 2018) or calcium sensors (Zhang et al., 2018) in combination with optogenetics. While *in vivo* recording and control of multiple cells using all-optical approaches can be very powerful for establishing the relationship between neuronal dynamics and behavior, in the case of calcium sensors, the response time of the sensors is on the order of tens to hundreds of milliseconds (Badura et al., 2014), which is too slow to enable direct inference of cellular activity, especially action potentials, that occur on the order of a millisecond. Recently developed voltage sensors do exhibit millisecond resolution, but technical challenges related to imaging speed and depth currently limit their application to studies observing only a few cells at a time in superficial layers of cortical tissues *in vivo* (deeper brain regions like hippocampus can be imaged only after aspirating overlying brain structures, as done in Adam et al., 2019 and Piatkevich et al., 2019). Most importantly, control over the membrane voltage, as achieved by the voltage clamp in the patch clamp technique, is not possible yet with optical approaches. Thus, while all-optical approaches are ideally suited for characterizing population activity in the context of behavior, patch clamp technology, along with other methods that establish direct electrical contact between a cell and a probe, such as recently developed nano-pipette technology (Jayant et al., 2019, 2017), remains an important tool for studying functional and biophysical aspects of individual neurons. Patch clamp recordings can furthermore be combined with labeling approaches to study cellular morphology and anatomy (Cid & de la Prida, this issue) as well as with single-cell RNA sequencing to characterize gene expression patterns (*e.g.*, Patch-seq; Cadwell et al., 2017, 2016), enabling comprehensive profiling of individual neurons.

The patch clamp technique has thus found its use in a wide range of applications that span from the measurement of ionic currents through transmembrane channel proteins of denervated frog muscle fibers at its inception (Neher and Sakmann, 1976) to the characterization of identified cell types in the mammalian brain (Chen et al., 2015; Gentet et al., 2012, 2010; Pala and Petersen, 2015; van Welie et al., 2016) to functional studies of individual cells in brain disorders (Arispe et al., 1996; Dragicevic et al., 2015; Ibáñez-Sandoval et al., 2007; Nieweg et al., 2015). Similar to other techniques in the biological sciences that have become standardized tools, initial improvements of patch clamp technology that were focused on optimizing manual operations are now being followed by innovations enabling automation for better ease-of-use, reproducibility, throughput, and standardization. This review will describe the initial development of the patch clamp technique and recent advances in automation of the technique, both *in vitro* and *in vivo*.

2. Initial development of patch clamp technique *in vitro*

When the patch clamp technique was first developed by Neher and Sakmann in 1976, they used heat-polished pipettes with a tip diameter of 3–5 μm to measure the current from enzymatically cleaned cell membrane surfaces (Neher and Sakmann, 1976; Sakmann and Neher, 1984). To reduce noise due to the leakage shunt between the cell membrane and the bath, the pipette had to be pressed onto the surface of the cell membrane, forming an electrical seal with tens of MΩ resistance between the pipette tip and the membrane (Neher and Sakmann, 1976). It was later discovered that light suction applied to the pipette upon contact between the pipette tip and the cell membrane can increase the seal resistance to above a gigaohm (*i.e.*, result in a gigaseal; Hamill et al., 1981; Sigworth and Neher, 1980). This discovery was important, because it improved the recording quality of the patch clamp technique (Sakmann and Neher, 1984) and enabled the development of different recording configurations (Hamill et al., 1981). These configurations include cell-attached, whole-cell, outside-out, and inside-out, each of which is best suited for different experimental applications (for reviews on these configurations, see Hamill et al., 1981; Okada, 2012; Sakmann and Neher, 1984; Zhao et al., 2008).

The need for direct contact between the pipette tip and the cell membrane limited the use of the patch clamp technique to isolated cells that have their membranes exposed (*e.g.*, cultured cells on a dish), until it was discovered that neurons in mammalian brain slices can be patched after brief treatment of the tissue slices with proteolytic enzymes (Gray and Johnston, 1985). However, since proteolytic enzymes may damage the proteins on the cell membrane of interest, different approaches were sought and developed. To enable direct contact between the tip of a patch pipette and the tissue-covered cell membrane, these approaches implemented either a two-step process in which a separate, "cleaning" pipette was first used to remove the part of the tissue covering the cell body of interest (Edwards et al., 1989) or a one-step process in which positive pressure was applied to a patch pipette as it was penetrating the tissue and approaching the cell membrane (Blanton et al., 1989). The integration of differential interference contrast (DIC) optics was another major advancement for enabling patch clamping in brain slices, as the improved imaging quality offered by DIC-based microscopy enabled visually-guided patching of soma as well as dendrites of targeted neurons in mammalian brain slices (Stuart et al., 1993). DIC-based visually-guided patch clamping has become a standard method for studying neurons in brain slices. More recently, with the advent of genetically engineered mouse models, cell type-specific fluorescent labeling (*e.g.*, as available in transgenic mice) and fluorescence imaging (*e.g.*, using an epifluorescence microscope) have been successfully combined with patch clamping to investigate genetically-defined neuronal classes *in vitro* (*e.g.*, Ting et al., 2014).

3. Patch clamp recordings *in vivo*

Although brain slices preserve synaptic connections in the immediate vicinity of the cells of interest and enable investigation of neuronal activity in somewhat intact local circuits (*i.e.*, more preserved circuits compared to cell cultures), more physiologically relevant insights into the relationship between neural activity and higher order brain functions, such as sensory information processing, perception, and memory, can only be achieved in *in vivo* preparations. The first successful *in vivo* whole-cell patch clamp recordings were demonstrated in the visual cortex of live, anesthetized cats (Pei et al., 1991). Although these recordings were obtained with an "incomplete" seal (*i.e.*, the seal resistance was 100–300 MΩ), this work suggested the feasibility of obtaining successful whole-cell patch clamp recordings *in vivo*. Several years later, it was demonstrated that whole-cell patch clamp recordings can be obtained from awake, head-fixed and even freely-moving rodents (Margrie et al., 2002; Lee et al., 2009, 2006), establishing the patch clamp technique as an invaluable tool for correlating single neuron activity to higher order brain functions.

3.1. Blind patch clamp recordings

The first *in vivo* whole-cell patch clamp recordings were performed in a "blind" fashion. In this recording mode, the whole-cell configuration is achieved without any visualization of targeted neurons or patch pipettes. A patch pipette, with high positive pressure (100–200 mbar in Margrie et al., 2002; 500–800 mbar in Lee et al., 2009) being applied to its interior to prevent clogging or blockage, is inserted into the brain to

a target depth. Once at the target depth, the positive pressure is reduced (to ~25 to 35 mbar), and the patch pipette is sequentially moved down in small (2–3 μm) steps while monitoring the tip resistance. When the pipette tip makes contact with a cell membrane, an increase in the pipette resistance and a pulsation of the pipette current are observed. The amount of resistance increase can vary depending on the magnitude of positive pressure applied to the pipette interior while approaching the cell, with the pipette tip resistance becoming less sensitive to the distance between the pipette tip and the cell membrane at excessively high positive pressure levels (≥0.6 psi according to Desai et al., 2015). However, high positive pressure can also be beneficial, because it helps keep the pipette tip clean while approaching the cell, which then leads to better contact with the cell membrane and ultimately to low access resistance (*i.e.*, better recording quality). Once the encounter between the pipette tip and the cell membrane is confirmed by observing the resistance change, the pipette pressure is released and suction is applied to form a gigaseal, followed by short suction pulses leading to break-in of the membrane patch and the whole-cell configuration.

Advantages of the blind patch technique include its (theoretically) unlimited depth of recordings (since the targeted depth is not limited by optical constraints) and the relatively large working area above the preparation (Okada, 2012). While knowledge of the anatomical arrangement of various classes of cells in different brain areas allows one to enhance the probability of targeting specific cell types (*e.g.* layer V cortical neurons), on the whole, blind patching is not an ideal method for the investigation of specific cell types or cell classes, given that the pipette encounters neurons in a random fashion (Margrie et al., 2003).

3.2. Image-guided patch clamp recordings

To overcome the limitation of the blind approach described above, *in vivo* two-photon laser scanning microscopy, which enables imaging of fluorescence signals relatively deep in the intact brain (Denk et al., 1994; Helmchen and Denk, 2005; Svoboda et al., 1997), has been integrated with patch clamping. In a method called "two-photon targeted patching" (TPTP; Komai et al., 2006; Margrie et al., 2003), cells that are fluorescently labeled by the generation of transgenic mice (*e.g.*, Meyer et al., 2002) or by the injection of viral vectors (*e.g.*, Callaway, 2005; Komai et al., 2006) are visualized simultaneously with a fluorescent dye-filled patch pipette, using a two-photon microscope. To distinguish the patch pipette from the cells, a fluorescent dye that has a significantly different emission spectrum compared to that of fluorescently labeled cells is used to fill the pipette. Similar to the blind approach, the patch pipette for TPTP is first moved into the brain under high positive pressure (100–600 mbar depending on the concentration of pipette dye). Once the pipette tip is positioned near the region of interest, the positive pressure is reduced (to 20–40 mbar), and the pipette is navigated to the target cell under visual guidance. While approaching the cell, both the pipette tip and the cell are imaged continuously to track the location of the cell, which is displaced in response to the pipette movement (by ~2 μm on average in the transverse plane according to Suk et al., 2017), and to adjust the pipette tip position accordingly. The pipette tip can be moved laterally inside the brain while approaching the cell, but the amount of lateral movements is kept low (usually below 50–75 μm) to reduce potential damage to the brain tissue. The final approach to the cell involves either axial movement of the pipette (*i.e.*, diagonal movement along the pipette axis) to the center of the cell body or placement of the pipette tip above the center of the cell and subsequent vertical movement onto the cell membrane. Since two-photon imaging generally cannot provide the level of structural detail that DIC-based microscopes offer, the distance between the pipette tip and the cell membrane during the final approach is estimated using the changes in the pipette tip resistance, as done in the blind approach, in addition to the visual guidance. A schematic representation of a TPTP setup is shown in Fig. 1A (adapted from Fig. 1 in Komai et al., 2006), together with example dual-channel images of a targeted cell and a patch pipette in Fig. 1B (adapted from Fig. 2 in Margrie et al., 2003).

In a closely related method termed "shadow-patching" (Kitamura et al., 2008; Häusser and Margrie, 2014), the extracellular space in the wild-type brain is perfused with a fluorescent dye from a patch pipette, which enables the visualization of unlabeled cells as "shadows" and thus image-guided navigation of the patch pipette to these cells. Unlike TPTP, shadow-patching allows for direct visualization of "dimpling" of the cell membrane (*i.e.*, the formation of a small depression in the cell membrane due to the pipette tip pushing against it, which signals good contact ready for gigasealing) as a bubble of dye trapped on the cell membrane, which helps with timing of the pressure release and suction application for gigaseal formation. For both TPTP and shadow-patching, formation of a gigaseal and rupture of the membrane patch for the whole-cell configuration are performed using similar procedures as in the blind approach.

Compared to the blind approach, image-guided patching is limited to a relatively low depth (~500 μm) due to tissue scattering that limits the imaging depth of two-photon microscopy. The level of illumination used during patching also needs to be carefully controlled, as using high laser intensity to better visualize the pipette tip and the cell membrane comes at a cost of lower chance of successfully forming a gigaseal, potentially due to the cell membrane or the pipette solution being negatively impacted (Komai et al., 2006; Margrie et al., 2003; the maximum average laser intensity tolerable for sealing and patching is between 1 and 10 mW according to Margrie et al., 2003). Despite these limitations, image-guided patching has been shown to be extremely valuable for cell type-specific characterizations of neurons in the intact brain (Chen et al., 2015; Gentet et al., 2012, 2010; Pala and Petersen, 2015; van Welie et al., 2016). Recent advances in laser scanning microscopy that enable imaging deeper in the intact tissue (*e.g.*, three-photon microscopy described in Horton et al., 2013), combined with the development of improved fluorescent tags (*e.g.*, near-infrared fluorescent proteins described in Piatkevich et al., 2017), may further broaden the application of image-guided patching.

3.3. Challenges of patch clamp recordings in vivo

Despite its obvious value as a tool for characterizing the function of different cell types in neural circuits, the patch clamp technique has not yet become a routine method in biological sciences, because it requires a lot of skill and experience to perform in comparison to other technologies. Consequently, in particular in the case of *in vivo* patch clamp, the technique has been adopted only by a relatively small subset of electrophysiologists. Even for these experts, *in vivo* patching has relatively low data yield (for the blind approach, ~20 to 30% of pipettes used for patching result in the formation of gigaseal and whole-cell configuration, according to Lee et al., 2009; Margrie et al., 2002; for TPTP, it is ~10 to 20%, according to Margrie et al., 2003), further emphasizing the need for automated approaches to enable higher yield and throughput.

4. Automated patch clamp recordings

To facilitate the use of patch clamp as a standardized tool in biology, several attempts have been made to automate the sequential steps involved in using the technique, for both *in vitro* and *in vivo* preparations. Currently available automated systems and strategies have shown various levels of success at reproducing or even surpassing the quality, yield, and throughput of recordings performed by human experimentalists, and we describe them below.

4.1. Automated patch clamp recordings in vitro

Early efforts to automate the patch clamp technique led to the development of planar devices for *in vitro* recordings from cultured cells

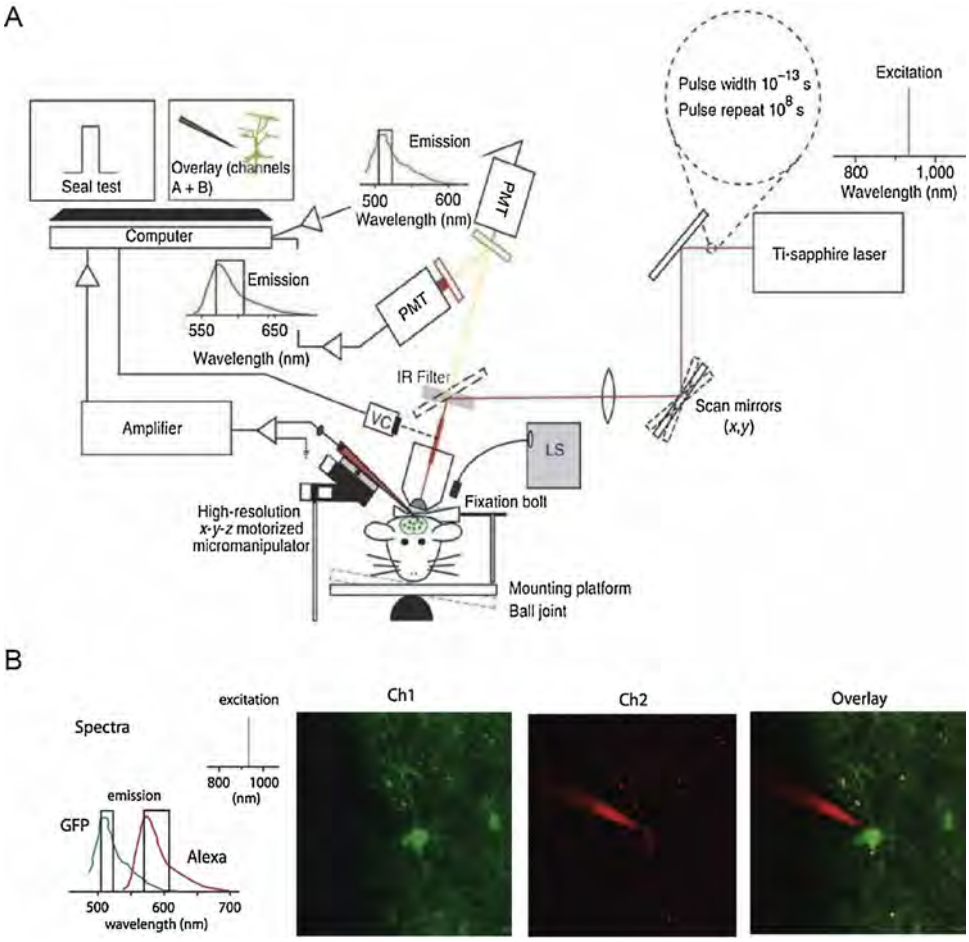

Fig. 1. (A) Schematic of a typical TPTP setup (adapted from Komai et al. (2006)). (B) Example dual-channel images of a targeted cell and a patch pipette (adapted from Margrie et al. (2003)).

(Dunlop et al., 2008; Okada, 2012). Instead of the "top-down" approach used in the manual recordings for the pipette-target cell contact formation, these automated systems use a "bottom-up" configuration (Dunlop et al., 2008), in which each well of a multi-well plate has a small aperture on the bottom surface. After the target cells in suspension are introduced into the wells of these systems, a negative pressure is applied through the apertures to bring the cells close and subsequently form a gigaseal. Although these systems enable automated patch clamp recordings with much higher throughput compared to the manual approach, the planar configuration limits their use to cells that can be isolated and suspended in a solution (for reviews on the automated patching systems with the planar configuration, see Dunlop et al., 2008 and Okada, 2012).

Automated systems that utilize conventional patch electrodes and sample preparations have also been developed. For example, the multi-electrode patch-clamp system developed by Perin and Markram (2013) is built around a conventional patch rig and simplifies multi-cell patching in brain slices by automating positioning of patch pipettes close to targeted cells. The system also provides a pneumatic system controlled by a human interface device for repeatable and precise pipette pressure adjustments during patching. However, several key steps are still left for human experimenters to perform (*e.g.*, the final approach to contact the cell with the pipette tip; triggering of pressure level adjustments for sealing and breaking in). With this system, twelve neurons could be patched simultaneously in brain slices of rats, far surpassing the number of cells that can be simultaneously patched using a fully manual approach (Perin and Markram, 2013).

To enable a near complete automation of image-guided patch clamp recordings in brain slices, a recent system termed the "Autopatcher IG" ("Image-Guided"; Wu et al., 2016) utilizes computer vision-based algorithms for automatic pipette tip calibration and fluorescent cell detection. The pipette tip calibration involves automatic detection of the location of the pipette tip that is imaged using an upright DIC-based microscope without fluorescence. Since commonly used fluorescence-based object and shape recognition strategies (*e.g.*, fluorescence intensity-based thresholding followed by shape or edge detection) cannot reliably detect non-fluorescent pipette tips, the Autopatcher IG addresses the challenge of pinpointing the position of the pipette tip by implementing a multi-stage image processing algorithm that involves de-noising, edge detection, feature extraction, and color inversion. This pipette tip detection strategy kept the positioning error low (1.6 μm on average) during automatic pipette tip calibration, which subsequently enabled automated pipette navigation to a targeted cell. The Autopatcher IG also automates seal formation and break-in, providing a platform for fully automated patching of fluorescent cells in brain slices. The system could be used to automate patching of fluorescent layer V neurons in cortical slices of Thy1-ChR2-EYFP mice, obtaining similar recording quality compared to manual patching of neurons in brain slices of wild-type mice. The average times spent for pipette positioning, gigaseal formation, and break-in were also significantly reduced compared to manual patching. For patching non-fluorescent cells in wild-type mice (which required manual cell detection using DIC optics), the system required user interruption during the patching process for 47.7% of the trials (21 out of 44 trials), mostly caused by inaccuracies in automated micromanipulator positioning or failure of the patching algorithm to form a gigaseal (Wu et al., 2016). For fully

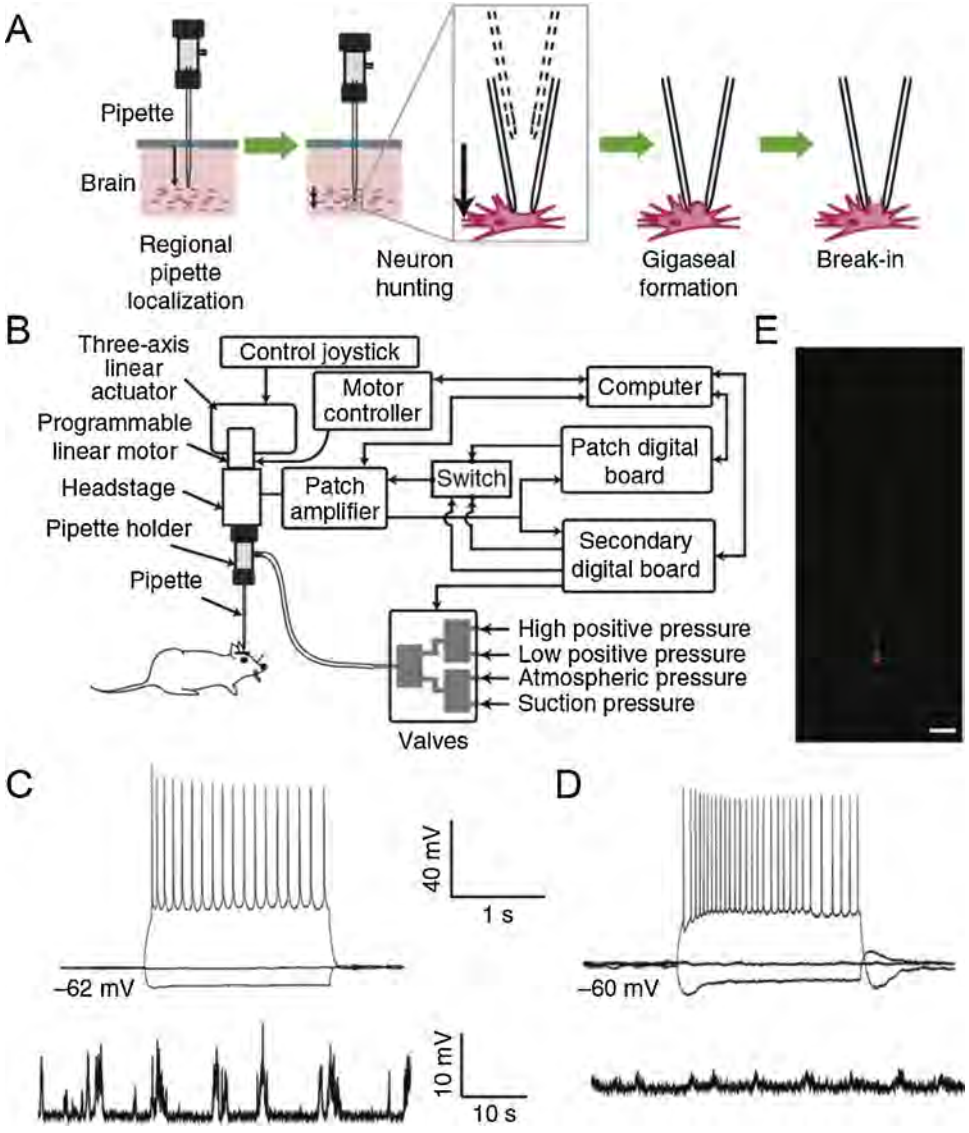

Fig. 2. Fig. 1 in Kodandaramaiah et al. (2012). (A) The autopatching algorithm. (B) Schematic of the autopatcher setup. (C) Example current-clamp recordings from an autopatched cortical neuron (top: recordings with 2-s long current injection pulses at −60, 0, and +80 pA; bottom: recording at rest). (D) Example current-clamp recordings from an autopatched hippocampal neuron (top: recordings with 2-s long current injection pulses at −60, 0, and +40 pA; bottom: recording at rest). (E) Example image of a biocytin-filled autopatched cortical neuron.

automated trials (which accounted for 23 out of 44 trials, or 52.3%) and semi-automated trials (*i.e.*, trials requiring user interruptions), the rates of achieving the successful whole-cell configuration (defined as a cell membrane resistance lower than 300 MΩ and a holding current between −200 pA and 100 pA) were 82.6% and 52.4% respectively, while it was 35.3% for manual trials. The seal resistance, the membrane capacitance, the membrane resistance, the access resistance, and the holding current were not significantly different between automatic/semi-automatic patching and manual patching, while the average times spent for pipette placement onto the target cell, gigaseal formation, and break-in were significantly shorter for automatic/semi-automatic patching compared to manual patching. While this was a major step towards full automation of slice patching, human intervention-free patch clamp recording of non-fluorescent cells visualized using DIC optics has not been achieved yet. As suggested by Wu et al., limitations that cause the Autopatcher IG to require user interruptions (as described above) could be potentially addressed by using micromanipulators with more accurate positioning capabilities and a closed-loop algorithm for continuous tracking of the pipette tip location, but a new image analysis strategy capable of detecting non-fluorescent cells and its implementation in the closed-loop algorithm for real-time tracking of the target cell position may be even more critical in overcoming the need for human intervention when using the Autopatcher IG.

4.2. Automated blind patch clamp recordings in vivo

The first automated system for *in vivo* patch clamp recordings was developed for blind patching (Kodandaramaiah et al., 2012). This LabVIEW-based system, called the “autopatcher”, utilizes an algorithm that divides the blind patching process into four distinct stages, as shown in Fig. 2A (Fig. 1(a) in Kodandaramaiah et al., 2012). To run this algorithm, the autopatcher integrates a set of standard patch clamp equipment, such as the pipette holder, the headstage, the patch amplifier, and the analog-to-digital converter, with programmable linear motors (for automated pipette navigation), computer-controlled pneumatic valves (for closed-loop pipette pressure modulation), and a digital board (for real-time pipette resistance measurement). Using the autopatcher, successful whole-cell recordings (defined as less than 500 pA of holding current when held at −65 mV for at least 5 min) could be

obtained from both cortical and hippocampal neurons in anesthetized mice at a rate of 32.9% (gigaseal cell-attached recordings were obtained 36% of the time), which is similar or superior to the success rates for manual *in vivo* patching reported in literature (Kodandaramaiah et al., 2012; Lee et al., 2009; Margrie et al., 2002). In addition, the quality of whole-cell recordings (assessed using access resistance, holding current, resting potential, and holding time) and the time required to obtain whole-cell recordings were similar between autopatching and manual *in vivo* patching (Kodandaramaiah et al., 2012; Lee et al., 2009; Margrie et al., 2002). It was later shown that the autopatcher could also be used to obtain whole-cell recordings from awake, head-fixed mice, either immobilized or running on a floating ball (Kodandaramaiah et al., 2016). Schematic representation of the autopatcher setup and example recordings obtained using the autopatcher are shown in Fig. 2B–D (Fig. 1(b)–(d) in Kodandaramaiah et al., 2012).

The autopatching algorithm has also been used to enable simultaneous patching of multiple cells (*i.e.*, multi-patching; Kodandaramaiah et al., 2018). The "multipatcher", composed of four interacting autopatching robots, could obtain dual or triple whole-cell recordings 30.7% of the time (*i.e.*, out of 41 trials, with four patch pipettes being simultaneously controlled in each trial, 13 trials led to two or three pipettes achieving the whole-cell configuration) in the visual and somatosensory cortices of anesthetized mice, but it could not obtain quadruple recordings. If each pipette is considered individually, the rate at which the whole-cell configuration could be obtained was 31.7% (52 out of 164 pipettes), which is similar to that reported for the autopatcher. When used in awake, head-fixed, body-restrained mice, the multipatcher led to at least one successful whole-cell recording in 55.7% of the trials and dual or triple recordings in 17.5% of the trials (which translated to the success rate of 17.3% when each pipette was considered individually).

A similar automated system was recently developed for blind patching in awake, head-fixed, behaving mice (Desai et al., 2015). This MATLAB-based system not only automates the key steps in blind patching, such as penetration of the dura, moving of the pipette tip to a targeted region, searching of a neuron, sealing, and break-in, but it also enables automatic positioning of patch pipettes into craniotomies before the start of the patching process, by integrating a camera and an image-processing algorithm. Using this system, successful whole-cell recordings could be typically obtained in 5 min at a rate of 17% in awake, head-fixed mice running on a wheel. The recording quality, as assessed using series resistance, was comparable to that obtained by manual patching, and the recording duration was 8 min on average (Desai et al., 2015). It is worth nothing that, although the success rate for the MATLAB-based system was lower compared to that for the autopatcher (17% *vs* 33%), the success rate for the multipatcher in awake, head-fixed mice was very close to that for the MATLAB-based system. The relatively low success rate may thus be mainly due to the added complexity involved in patching in awake animals (*e.g.*, significant and largely unpredictable brain movement due to locomotion) rather than the differences between the systems (*e.g.*, pressure levels used for patching, removal of dura).

To improve the yield of automated patch clamp recordings deep in the brain (*e.g.*, in the thalamus), a robotic system that adds automatic lateral pipette navigation to the autopatching algorithm was recently developed (Stoy et al., 2017). As the pipette penetrates the brain to reach a desired region/depth for patching, the system detects an obstruction (*e.g.*, a blood vessel) by detecting an increase in the pipette tip resistance ($\geq$12.5% increase above baseline resistance). Once an obstruction is encountered, the pipette tip is retracted parallel to the pipette axis and the pipette tip resistance is subsequently recorded to establish a baseline value. The pipette tip is then moved laterally, lowered back to the depth at which the obstruction was detected, and the pipette tip resistance is checked again to determine if the tip resistance is less than 200 kΩ above the baseline value (in which case, it is presumed that the tip has successfully circumvented the obstruction). If the pipette tip still shows a resistance increase above the threshold value, the steps described above are repeated until the resistance increase is below the threshold or the lateral excursion exceeds 50 µm. Using this "dodging algorithm", the rate of clogging the pipette tip while moving the pipette tip to the depth of 3000 µm in the mouse brain was drastically reduced (from around 75% to 18%), but the time it took to reach the target depth was also significantly increased (from 6 s to 75 s). The autopatcher implementing the dodging algorithm could obtain whole-cell recordings from neurons in the thalamus, with access resistance, holding currents, and resting membrane potentials that were comparable to those from cortical neurons. The success rate for a whole-cell recording from a thalamic neuron was 10%, which was a ten-fold improvement compared to that obtained without using the automatic lateral pipette navigation for dodging obstruction (Stoy et al., 2017). However, a success rate of 10% in anesthetized mice is still much lower compared to that achievable in the cortex and hippocampus using the autopatcher, and it would need to be improved for this strategy to become a practical way of recording from deep brain structures. As suggested by Stoy et al., strategies for improving the placement of the pipette tip on the cell membrane, such as mapping of the target cell morphology by using the patch pipette as the probe for scanning ion conductance microscopy and estimation of membrane dimpling by observing changes in the pipette tip resistance in response to pressure modulation (Sánchez et al., 2008), may help increase the success rate for automated recordings in deeper tissues.

4.3. Automated image-guided patch clamp recordings in vivo

One of the first attempts at automating image-guided patching *in vivo* has resulted in a system called "smartACT" (smart Adaptive Cell Targeting), which enables automatic positioning of a patch pipette close to a targeted cell (Long et al., 2015). In the initial stages of its workflow, in which the pipette tip is positioned above the brain surface, smartACT utilizes 3D volume rendering of a two-photon image stack to allow for the selection of the pipette tip and target cell locations by a user. Once the pipette tip is automatically moved into the brain and placed at a certain distance away from the target cell, the system acquires another image stack and performs image segmentation on it to achieve automatic detection of the pipette tip and the target cell. The detection of the pipette tip and target cell locations enables adaptive adjustments of the pipette trajectory, resulting in a more accurate positioning of the pipette tip near the target cell. A user is then responsible for making the final approach to the cell, establishing contact with the cell membrane, gigasealing, and rupturing the cell membrane for whole-cell recordings. Using smartACT, the pipette tip could be moved from outside the brain to near a target cell in a similar time as a human experimenter, and manual patching following this automated pipette positioning led to whole-cell recordings in the primary visual cortex of anesthetized mice, with patched neurons showing electrophysiological characteristics similar to those in literature (Long et al., 2015).

A near complete automation of image-guided patching *in vivo* was reported recently by two groups (Annecchino et al., 2017; Suk et al., 2017). The systems developed by these groups are both built on a commercial two-photon microscope and utilize a custom-built pressure controller. They also use a similar approach to compensate for the movement of a target cell while navigating a patch pipette toward it; namely, a closed-loop real-time imaging strategy in which the target cell location is continuously updated and the pipette trajectory is subsequently adjusted to achieve accurate positioning of the pipette tip onto the target cell. With the ability to address the key technical challenge of compensating for the target cell movement during targeted patching, both systems could automate all of the key steps involved in image-guided patching *in vivo*, which include pipette positioning into the brain and onto a target cell, gigaseal formation, and break-in. Schematic representations of the algorithms and the hardware of the system developed by Suk et al., termed the "imagepatcher", are shown

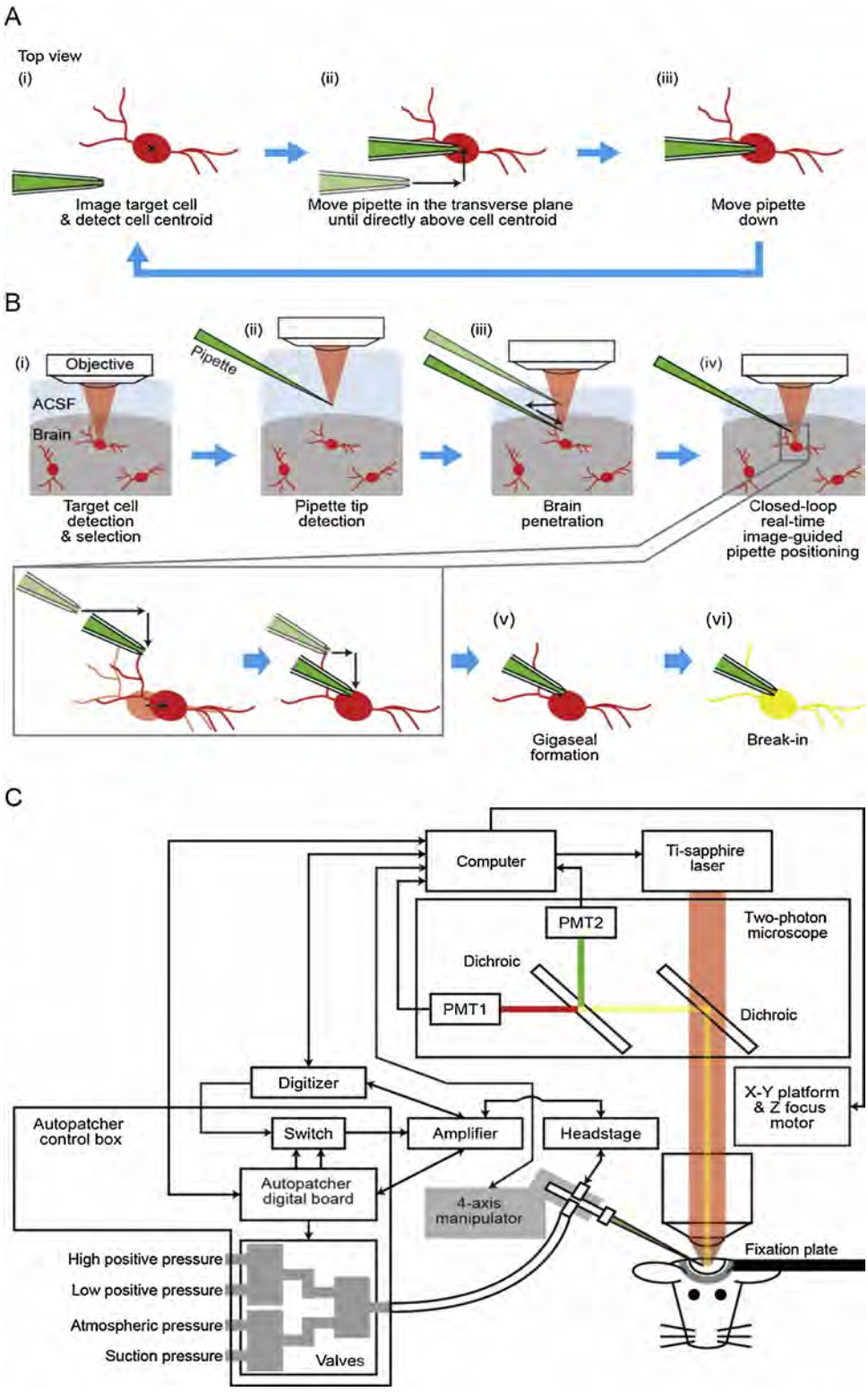

Fig. 3. Overview of the imagepatcher. (A) The closed-loop algorithm for continuous cell centroid localization and pipette position adjustment while approaching the targeted cell. (B) The image-guided automated patching algorithm. (C) Schematic of the imagepatcher hardware. Figures adapted from Fig. 1 in Suk et al. (2017).

in Fig. 3 (adapted from Fig. 1 in Suk et al., 2017).

When targeting cortical PV-positive neurons in anesthetized mice, the performance of the two systems was quite similar: the success rates for a gigaseal and the whole-cell configuration reported by Suk et al. were 38.9% and 22.2% respectively (in PV-Cre x Ai14 mice), and those reported by Annecchino et al. were 46.6% and 22.2% respectively (in GAD67-GFP mice); the time it took to achieve the whole-cell configuration was 10 ± 3 min for Suk et al. and 6 ± 1 min for Annecchino et al. Both systems also reported quality of recordings and electrophysiological characteristics of their patched cells that were similar to those obtained from manually patched cortical neurons. In addition to PV-positive neurons, the system by Suk et al. could be used to patch targeted cortical CaMKIIα-positive neurons (in CaMKIIα-Cre x Ai14 mice), achieving a gigaseal 29.2% of the time and the whole-cell

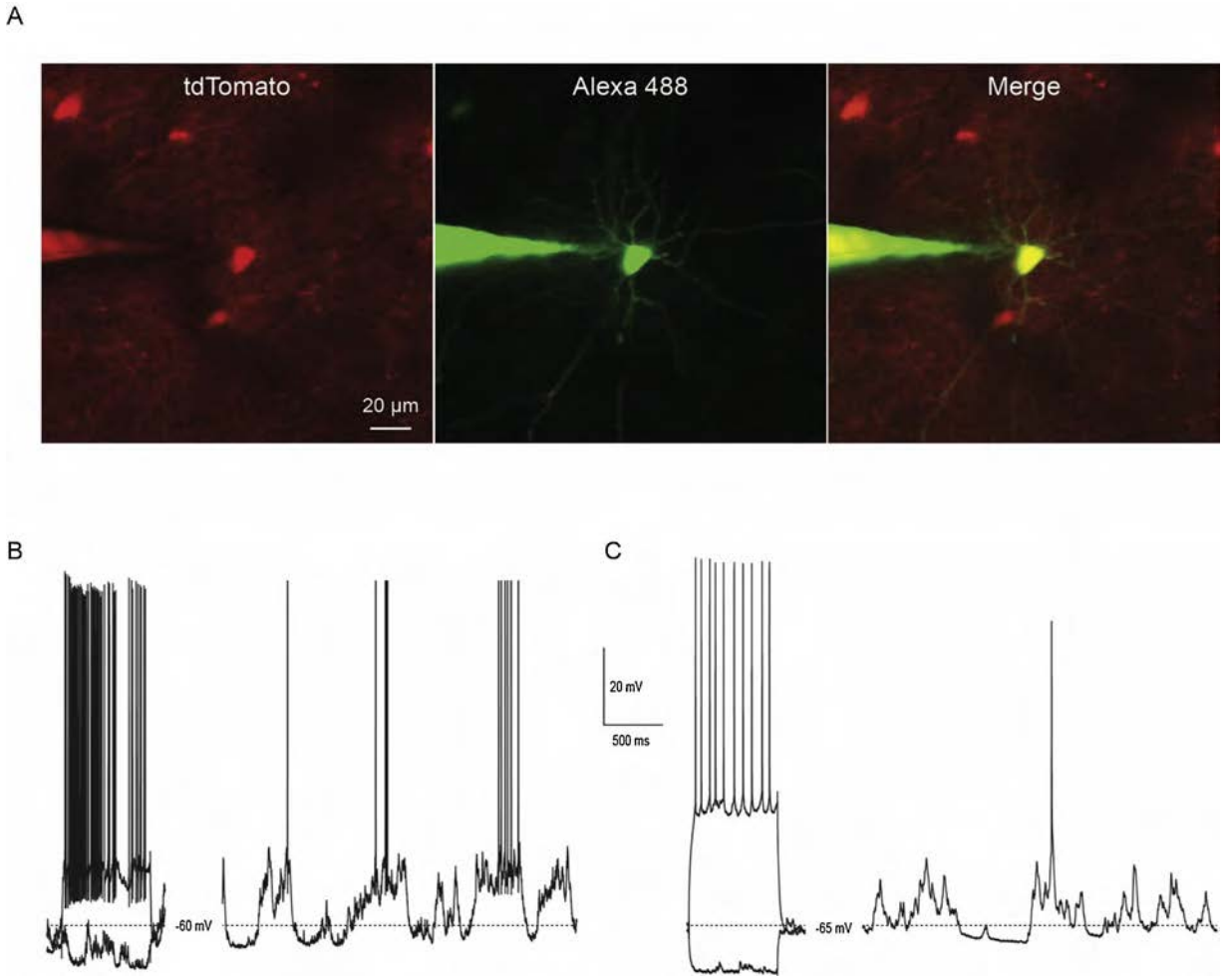

Fig. 4. (A) Example dual-channel images of an imagepatched cortical PV-positive neuron (Fig. 3D in Suk et al. (2017)). (B) Example whole-cell current-clamp recordings from an imagepatched cortical PV-positive neuron (left: recordings with current injection pulses at −100 and +200 pA; right: recording at rest; Fig. 4E in Suk et al. (2017)). (C) Example whole-cell current-clamp recordings from an imagepatched cortical CaMKIIα-positive neuron (left: recordings with current injection pulses at −100 and +200 pA; right: recording at rest; Fig. 4F in Suk et al. (2017)).

recording 20.0% of the time. Annecchino et al. also showed their system could be used to patch targeted Purkinje cells in the cerebellum of GAD67-GFP mice as well as cortical pyramidal neurons and astrocytes in wild-type mice that were labeled using bulk loading of either Oregon Green BAPTA-1 AM or Sulforhodamine-101. Example images of an imagepatched cortical neuron and whole-cell recordings obtained using the imagepatcher are shown in Fig. 4 (adapted from Fig. 3D, 4 E and F in Suk et al., 2017).

Among these similarities, some differences between the two systems exist. For example, the system by Suk et al. makes the final approach to the target cell (*i.e.* in the last ~10 to 15 µm) in the z-direction (*i.e.*, vertically) while the final step taken towards the cell is purely axial (*i.e.* parallel to the pipette axis) in the system by Annecchino et al. It has to be noted that both of these approaches have been used in manual image-guided patching *in vivo* (Häusser and Margrie, 2014; Komai et al., 2006; Margrie et al., 2003), and to our knowledge, it has not been reported that these approaches have a differential effect on the brain tissue or patch-clamp recordings. Another difference between the two systems is that while Suk et al. uses a pipette tip detection algorithm to automatically locate the pipette tip outside the brain and navigate the tip close to the brain surface, Annecchino et al. relies on a user to determine the pipette tip location and manually position the tip before penetrating the brain. Finally, in the event that the automatic closed-loop navigation of a pipette does not result in contact with a target cell, the system by Annecchino et al. requires manual adjustments of the pipette position, while the system by Suk et al. automatically retracts the pipette, updates the target cell location, and resumes the automatic closed-loop approach to the target cell (up to a set number of times).

While these two systems work well and show yield levels that are similar to or slightly better than that of manual approaches, there are still some manual steps involved. The requirement for a two-photon microscope, which is expensive, is also a hurdle for a widespread adoption of automated two-photon image-guided patching. However, the biggest advantage of using an automated system is arguably the mitigation of the time and effort required to learn the skill of manual patching; while an experimenter experienced in *in vitro* patch clamping may pick up the necessary skills for *in vivo* image-guided patch clamping fairly quickly, the time required for a novice to learn the technique can be substantial, at least around 4–6 months on average based on our experience. These automated systems should therefore considerably lower the bar for experimenters who are new to *in vivo* patch clamp, but want to obtain image-guided patch clamp recordings *in vivo* for their studies within a reasonable time-frame.

5. Future directions in the automation of whole-cell patch clamp

Automation of patch clamp technology, especially *in vivo* patch clamp, has made tremendous strides in recent years as described above. The autopatcher has been used to help characterize and validate a new non-invasive deep brain stimulation technique (Grossman et al., 2017)

and to study membrane voltage changes in awake animals (Kolb et al., 2018; Singer et al., 2017), but it has yet to be widely adopted across different laboratories. Notably, several steps in the *in vivo* patch clamp procedure are still manual, including pipette pulling, pipette exchanging, and pipette positioning under the objective. Recently, an interesting advance towards easing pipette exchanging was made (Kolb et al., 2016). This study describes a method that utilizes an enzymatic detergent (Alconox) to clean pipettes after use, enabling re-use within one minute of retraction. While pipettes appeared to be sufficiently cleaned using this method to allow for re-use, any potential negative side effects of any potential residual Alconox on cellular functions remain to be established. Another approach taken towards easing pipette exchanging includes the use of a carousal loaded with pulled pipettes, but this approach led to a very low yield of successful recordings (9%), potentially due to contamination and clogging of loaded pipettes (Holst et al., 2019). Combining an automated pressure control system similar to that implemented in the autopatcher with automated pipette cleaning in customized chambers has recently allowed one group to successfully achieve high yield multi-patch (up to 10 manipulators) experiments in rodent and human brain slices (Peng et al., 2019). For now, it remains to be seen how easily the cleaning approach can be integrated with *in vivo* patch setups, which tend to have many space constraints directly around the mouse holder and manipulators, especially in the case of two-photon image-guided patch clamp experiments.

Another major step that is still fully manual in the automated approaches mentioned above is that of performing a craniotomy (*i.e.* the procedure of drilling a hole in the skull for pipette access). Especially for image-guided patching, a perfect craniotomy without damage to blood vessels and brain tissue is crucial for successful patch clamp recordings, but it is difficult to perform and it requires much training to learn to perform a perfect craniotomy. For small craniotomies generally used in blind patching, it was found that this challenging procedure can be automated by measuring the electrical conductance at the tip of the drill while it is drilling into the skull (Pak et al., 2015). With an algorithm that uses an increase in the drill tip conductance to determine the moment a drill bit passes through the bottom of the skull, a robotic system that can make single or multiple craniotomies of various sizes was developed. This system was originally integrated with a commercial motorized stereotaxic instrument (Neurostar) to enable stereotaxically targeted drilling (Pak et al., 2015), and Neurostar now offers a stereotaxic with the robotic drill as an add-on. A more recent approach utilizes an actuation sensor to profile the 3D shape of a mouse's skull, which is then used to guide a modified desktop computer numerical controlled (CNC) mill to drill desired drilling patterns, from skull thinning to drilling holes for bone anchor screws to drilling large craniotomies, as used for image-guided patch clamp (Ghanbari et al., 2019b). These automated craniotomy systems may be integrated with automated patching systems to circumvent the need to perform craniotomies manually.

In addition to performing a craniotomy, an important step in *in vivo* image-guided patching is performing a durotomy (*i.e.*, the process of removing the dura), which follows the craniotomy. In blind patching, the durotomy is not as critical, as patch pipettes often enter the brain through the same spot on the brain surface, which increases the chance of making a hole through the dura, even if left intact, and thus prevents the clogging of pipette tips in subsequent trials. With image-guided patching however, the pipette tip does not necessarily enter the brain through the same spot on the brain surface each time, which means the dura may need to be pierced anew at a different location with each pipette penetration. Each trial therefore faces a high chance of clogging the pipette tip. It is thus important to remove the entire dura (or at least a significant portion of the dura) found in the craniotomy for image-guided patching. However, similar to performing a craniotomy, performing a durotomy with minimal damage to the underlying tissue is difficult and requires a lot of training of the experimenter to be done well. Future approaches to standardize or automate durotomy procedures may evolve around enzymatic dissolution of the dura or the use of optical tools that may visualize the dura better than is currently feasible using standard light microscopy.

The most crucial problem that is encountered during *in vivo* image-guided patch clamp experiments in awake animals is movement of the brain inside a large craniotomy. Experimenters who routinely perform chronic imaging experiments have mitigated this issue by implanting a small glass coverslip after a craniotomy is performed. Also, attempts have even been made to replace the entire skull above the cortex with glass (Kim et al., 2016) or with polymer skulls (Ghanbari et al., 2019a). Chronic image-guided patch clamp experiments may be enabled by a similar approach of gaining optical access to a large extent of the brain, combined with (sterotaxically autodrilled) holes for pipette entry. While not designed with image-guided patch clamp experiments in mind, a method for drilling holes through glass coverslips implanted for chronic imaging has been already described (Roome and Kuhn, 2018). It therefore seems theoretically feasible that, in the near future, glass skulls that minimize brain movement could be penetrated at desired locations using an automated drilling approach. These locations can then be utilized by an automated patch clamp system for patching targeted cells through these holes, allowing for fully automated image-guided patch clamp recordings in awake animals.

While *in vivo* patch clamp is the ideal approach for studying neural activity in relation to sensory and/or motor functions in behaving animals, especially in combination with optogenetics and/or pharmacological approaches (Katz et al., this issue), *in vitro* patch clamp is still an extremely valuable tool to study cell-type specific biophysics, connectivity between cell types, and pharmacology of ion channels. A great opportunity therefore exists in further automating *in vitro* patch clamp technology. Given the advances in automating *in vivo* patch clamp, it should be feasible to fully automate patch clamping of fluorescent cells in brain slices. However, the automation of patching non-labeled neurons visualized with DIC optics is less straightforward and may require further breakthroughs in image-analysis of non-fluorescent structures. A recent development of a system named the "Patcherbot" (Kolb et al., 2019) is a potentially useful step towards this goal. The Patcherbot uses a machine-learning algorithm to track and correct for the movement of target cells in brain slices imaged using DIC optics; the cells are initially identified by a human experimenter, but are then tracked by the "cell tracker" algorithm that delineates the outline of the cells. A method for fully automated visual identification of cell bodies in DIC images without initial user selection has yet to be reported, but the strategy introduced by the Patcherbot holds promise for future progress in truly human-free, unattended *in vitro* patch clamp recordings.

Finally, one important aspect of patch clamp recordings that is not addressed in any of the automated systems above is the fact that unlike most other wet-bench technologies, a certain degree of real time data interpretation by the experimenter is crucial during patch clamp experiments. While some aspects related to the quality of recordings (*e.g.*, seal resistance, access resistance) are already monitored in an automated fashion by some of the systems described above, experimental patch clampers often make changes to both the experimental conditions (*e.g.*, pipette pressure, pipette tip positioning) and the applied protocols used for current or voltage clamp during recordings based on the real-time findings. Indeed, many important discoveries related to biophysical properties have been made by real time interpretation of the data being recorded and subsequent manipulation of experimental conditions and/or protocols. This illustrates that automation of patch clamp technology may be mostly useful for experiments requiring large datasets generated from rigid and standard protocols, such as those used during drug screening or basic cellular characterizations. For biological discoveries to be made from patch clamp recordings, real-time human insight and judgement will remain crucially important.

Acknowledgements

Our work on automation of targeted patch clamp was supported by Jeremy and Joyce Wertheimer, NIH 1R01NS102727, NIH 1R01EY023173, NIH 1R01MH103910, NIH Director's Pioneer Award1DP1NS087724, the MIT Synthetic Intelligence Project, the MIT Media Lab, the HHMI-Simons Faculty Scholars Program, and the New York Stem Cell Foundation–Robertson Award and a Samsung Scholarship.

References

Adam, Y., Kim, J.J., Lou, S., Zhao, Y., Xie, M.E., Brinks, D., Wu, H., Mostajo-Radji, M.A., Kheifets, S., Parot, V., Chettih, S., Williams, K.J., Gmeiner, B., Farhi, S.L., Madisen, L., Buchanan, E.K., Kinsella, I., Zhou, D., Paninski, L., Harvey, C.D., Zeng, H., Arlotta, P., Campbell, R.E., Cohen, A.E., 2019. Voltage imaging and optogenetics reveal behaviour-dependent changes in hippocampal dynamics. Nature 569, 413–417. https://doi.org/10.1038/s41586-019-1166-7.

Annecchino, L.A., Morris, A.R., Copeland, C.S., Agabi, O.E., Chadderton, P., Schultz, S.R., 2017. Robotic automation of in vivo two-photon targeted whole-cell patch-clamp electrophysiology. Neuron 95, 1048–1055. https://doi.org/10.1016/j.neuron.2017.08.018. e3.

Arispe, N., Pollard, H.B., Rojas, E., 1996. Zn2+ interaction with Alzheimer amyloid beta protein calcium channels. Proc. Natl. Acad. Sci. U. S. A. 93, 1710–1715. https://doi.org/10.1073/PNAS.93.4.1710.

Badura, A., Sun, X.R., Giovannucci, A., Lynch, L.A., Wang, S.S.-H., 2014. Fast calcium sensor proteins for monitoring neural activity. Neurophotonics 1https://doi.org/10.1117/1.NPh.1.2.025008. 025008.

Blanton, M.G., Lo Turco, J.J., Kriegstein, A.R., 1989. Whole cell recording from neurons in slices of reptilian and mammalian cerebral cortex. J. Neurosci. Methods 30, 203–210. https://doi.org/10.1016/0165-0270(89)90131-3.

Cadwell, C.R., Palasantza, A., Jiang, X., Berens, P., Deng, Q., Yilmaz, M., Reimer, J., Shen, S., Bethge, M., Tolias, K.F., Sandberg, R., Tolias, A.S., 2016. Electrophysiological, transcriptomic and morphologic profiling of single neurons using Patch-seq. Nat. Biotechnol. 34, 199–203. https://doi.org/10.1038/nbt.3445.

Cadwell, C.R., Scala, F., Li, S., Livrizzi, G., Shen, S., Sandberg, R., Jiang, X., Tolias, A.S., 2017. Multimodal profiling of single-cell morphology, electrophysiology, and gene expression using Patch-seq. Nat. Protoc. 12, 2531–2553. https://doi.org/10.1038/nprot.2017.120.

Callaway, E.M., 2005. A molecular and genetic arsenal for systems neuroscience. Trends Neurosci. https://doi.org/10.1016/j.tins.2005.01.007.

Chen, I.-W., Helmchen, F., Lutcke, H., 2015. Specific early and late oddball-evoked responses in excitatory and inhibitory neurons of mouse auditory cortex. J. Neurosci. 35, 12560–12573. https://doi.org/10.1523/JNEUROSCI.2240-15.2015.

Denk, W., Delaney, K.R., Gelperin, A., Kleinfeld, D., Strowbridge, B.W., Tank, D.W., Yuste, R., 1994. Anatomical and functional imaging of neurons using 2-photon laser scanning microscopy. J. Neurosci. Methods 54, 151–162. https://doi.org/10.1016/0165-0270(94)90189-9.

Desai, N.S., Siegel, J.J., Taylor, W., Chitwood, R.A., Johnston, D., 2015. MATLAB-based automated patch-clamp system for awake behaving mice. J. Neurophysiol. 114, 1331–1345. https://doi.org/10.1152/jn.00025.2015.

Dragicevic, E., Schiemann, J., Liss, B., 2015. Dopamine midbrain neurons in health and Parkinson's disease: emerging roles of voltage-gated calcium channels and ATP-sensitive potassium channels. Neuroscience 284, 798–814. https://doi.org/10.1016/j.neuroscience.2014.10.037.

Dunlop, J., Bowlby, M., Peri, R., Vasilyev, D., Arias, R., 2008. High-throughput electrophysiology: an emerging paradigm for ion-channel screening and physiology. Nat. Rev. Drug Discov. 7, 358–368. https://doi.org/10.1038/nrd2552.

Edwards, F.A., Konnerth, A., Sakmann, B., Takahashi, T., 1989. A thin slice preparation for patch clamp recordings from neurones of the mammalian central nervous system. Pflügers Arch. Eur. J. Physiol. 414, 600–612. https://doi.org/10.1007/BF00580998.

Gentet, L.J., Avermann, M., Matyas, F., Staiger, J.F., Petersen, C.C.H., 2010. Membrane potential dynamics of GABAergic neurons in the barrel cortex of behaving mice. Neuron 65, 422–435. https://doi.org/10.1016/j.neuron.2010.01.006.

Gentet, L.J., Kremer, Y., Taniguchi, H., Huang, Z.J., Staiger, J.F., Petersen, C.C., 2012. Unique functional properties of somatostatin-expressing GABAergic neurons in mouse barrel cortex. Nat. Neurosci. 15, 607–612. https://doi.org/10.1038/nn.3051.

Ghanbari, L., Carter, R.E., Rynes, M.L., Dominguez, J., Chen, G., Naik, A., Hu, J., Sagar, M.A.K., Haltom, L., Mossazghi, N., Gray, M.M., West, S.L., Eliceiri, K.W., Ebner, T.J., Kodandaramaiah, S.B., 2019a. Cortex-wide neural interfacing via transparent polymer skulls. Nat. Commun. 10, 1500. https://doi.org/10.1038/s41467-019-09488-0.

Ghanbari, L., Rynes, M.L., Hu, J., Schulman, D.S., Johnson, G.W., Laroque, M., Shull, G.M., Kodandaramaiah, S.B., 2019b. Craniobot: a computer numerical controlled robot for cranial microsurgeries. Sci. Rep. 9, 1023. https://doi.org/10.1038/s41598-018-37073-w.

Gray, R., Johnston, D., 1985. Rectification of single GABA-gated chloride channels in adult hippocampal neurons. J. Neurophysiol. 54, 134–142. https://doi.org/10.1152/jn.1985.54.1.134.

Grossman, N., Bono, D., Dedic, N., Kodandaramaiah, S.B., Rudenko, A., Suk, H.J., Cassara, A.M., Neufeld, E., Kuster, N., Tsai, L.H., Pascual-Leone, A., Boyden, E.S., 2017. Noninvasive deep brain stimulation via temporally interfering electric fields. Cell 169, 1029–1041. https://doi.org/10.1016/j.cell.2017.05.024. e16.

Hamill, O.P., Marty, A., Neher, E., Sakmann, B., Sigworth, F.J., 1981. Improved patch-clamp techniques for high-resolution current recording from cells and cell-free membrane patches. Pflügers Arch. Eur. J. Physiol. 391, 85–100. https://doi.org/10.1007/BF00656997.

Häusser, M., Margrie, T.W., 2014. Two-photon targeted patching and electroporation in vivo. Cold Spring Harb. Protoc. 2014, 78–85. https://doi.org/10.1101/pdb.prot080143.

Helmchen, F., Denk, W., 2005. Deep tissue two-photon microscopy. Nat. Methods 2, 932–940. https://doi.org/10.1038/nmeth818.

Hochbaum, D.R., Zhao, Y., Farhi, S.L., Klapoetke, N., Werley, C.A., Kapoor, V., Zou, P., Kralj, J.M., MacLaurin, D., Smedemark-Margulies, N., Saulnier, J.L., Boulting, G.L., Straub, C., Cho, Y.K., Melkonian, M., Wong, G.K.S., Harrison, D.J., Murthy, V.N., Sabatini, B.L., Boyden, E.S., Campbell, R.E., Cohen, A.E., 2014. All-optical electrophysiology in mammalian neurons using engineered microbial rhodopsins. Nat. Methods 11, 825–833. https://doi.org/10.1038/NMETH.3000.

Holst, G., Stoy, W.A., Yang, B., Kolb, I., Kodandaramaiah, S.B., Li, L., Knoblich, U., Zeng, H., Haider, B., Boyden, E.S., Forest, C.R., 2019. Autonomous patch clamp robot for functional characterization of neurons in vivo: development and application to mouse visual cortex. J. Neurophysiol. 121, 2341–2357. https://doi.org/10.1152/jn.00738.2018.

Horton, N.G., Wang, K., Wang, C.C., Xu, C., 2013. In vivo three-photon imaging of subcortical structures of an intact mouse brain using quantum dots. 2013 Conf. Lasers Electro-Optics Eur. Int. Quantum Electron. Conf. CLEO/Europe-IQEC 2013 7 205–209. https://doi.org/10.1109/CLEOE-IQEC.2013.6801501.

Ibáñez-Sandoval, O., Carrillo-Reid, L., Galarraga, E., Tapia, D., Mendoza, E., Gomora, J.C., Aceves, J., Bargas, J., 2007. Bursting in substantia Nigra pars reticulata neurons in vitro: possible relevance for Parkinson disease. J. Neurophysiol. 98, 2311–2323. https://doi.org/10.1152/jn.00620.2007.

Jayant, K., Hirtz, J.J., La Plante, I.J., Tsai, D.M., De Boer, W.D.A.M., Semonche, A., Peterka, D.S., Owen, J.S., Sahin, O., Shepard, K.L., Yuste, R., 2017. Targeted intracellular voltage recordings from dendritic spines using quantum-dot-coated nanopipettes. Nat. Nanotechnol. 12, 335–342. https://doi.org/10.1038/nnano.2016.268.

Jayant, K., Wenzel, M., Bando, Y., Hamm, J.P., Mandriota, N., Rabinowitz, J.H., La Plante, I.J., Owen, J.S., Sahin, O., Shepard, K.L., Yuste, R., 2019. Flexible nanopipettes for minimally invasive intracellular electrophysiology in vivo. Cell Rep. 26, 266–278. https://doi.org/10.1016/j.celrep.2018.12.019. e5.

Kim, T.H., Zhang, Y., Lecoq, J., Jung, J.C., Li, J., Zeng, H., Niell, C.M., Schnitzer, M.J., 2016. Long-term optical access to an estimated one million neurons in the live mouse cortex. Cell Rep. 17, 3385–3394. https://doi.org/10.1016/j.celrep.2016.12.004.

Kiskinis, E., Kralj, J.M., Zou, P., Weinstein, E.N., Zhang, H., Tsioras, K., Wiskow, O., Ortega, J.A., Eggan, K., Cohen, A.E., 2018. All-optical electrophysiology for high-throughput functional characterization of a human iPSC-derived motor neuron model of ALS. Stem Cell Rep. 10, 1991–2004. https://doi.org/10.1016/j.stemcr.2018.04.020.

Kitamura, K., Judkewitz, B., Kano, M., Denk, W., Hausser, M., 2008. Targeted patch-clamp recordings and single-cell electroporation of unlabeled neurons in vivo. Nat. Methods 5, 61–67. https://doi.org/10.1038/nmeth1150.

Kodandaramaiah, S.B., Flores, F.J., Holst, G.L., Singer, A.C., Han, X., Brown, E.N., Boyden, E.S., Forest, C.R., 2018. Multi-neuron intracellular recording in vivo via interacting autopatching robots. Elife 7https://doi.org/10.7554/eLife.24656. e24656.

Kodandaramaiah, S.B., Franzesi, G.T., Chow, B.Y., Boyden, E.S., Forest, C.R., 2012. Automated whole-cell patch-clamp electrophysiology of neurons in vivo. Nat. Methods. https://doi.org/10.1038/nmeth.1993.

Kodandaramaiah, S.B., Holst, G.L., Wickersham, I.R., Singer, A.C., Franzesi, G.T., McKinnon, M.L., Forest, C.R., Boyden, E.S., 2016. Assembly and operation of the autopatcher for automated intracellular neural recording in vivo. Nat. Protoc. 11, 634–654. https://doi.org/10.1038/nprot.2016.007.

Kolb, I., Landry, C.R., Yip, M.C., Lewallen, C.F., Stoy, W.A., Lee, J., Felouzis, A., Yang, B., Boyden, E.S., Rozell, C.J., Forest, C.R., 2019. PatcherBot: a single-cell electrophysiology robot for adherent cells and brain slices. J. Neural Eng. 16https://doi.org/10.1088/1741-2552/ab1834. 046003.

Kolb, I., Stoy, W.A., Rousseau, E.B., Moody, O.A., Jenkins, A., Forest, C.R., 2016. Cleaning patch-clamp pipettes for immediate reuse. Sci. Rep. 6, 35001. https://doi.org/10.1038/srep35001.

Kolb, I., Talei Franzesi, G., Wang, M., Kodandaramaiah, S.B., Forest, C.R., Boyden, E.S., Singer, A.C., 2018. Evidence for long-timescale patterns of synaptic inputs in CA1 of awake behaving mice. J. Neurosci. 38, 1821–1834. https://doi.org/10.1523/JNEUROSCI.1519-17.2017.

Komai, S., Denk, W., Osten, P., Brecht, M., Margrie, T., 2006. Two-photon targeted patching (TPTP) in vivo. Nat. Protoc. 1, 647–652. https://doi.org/10.1038/nprot.2006.100.

Lee, A.K., Epsztein, J., Brecht, M., 2009. Head-anchored whole-cell recordings in freely moving rats. Nat. Protoc. 4, 385–392. https://doi.org/10.1038/nprot.2009.5.

Lee, A.K., Manns, I.D., Sakmann, B., Brecht, M., 2006. Whole-cell recordings in freely moving rats. Neuron 51, 399–407. https://doi.org/10.1016/j.neuron.2006.07.004.

Long, B., Li, L., Knoblich, U., Zeng, H., Peng, H., 2015. 3D image-guided automatic pipette positioning for single cell experiments in vivo. Sci. Rep. 5, 18426. https://doi.org/10.1038/srep18426.

Margrie, T.W., Brecht, M., Sakmann, B., 2002. In vivo, low-resistance, whole-cell recordings from neurons in the anaesthetized and awake mammalian brain. Pflugers Arch. Eur. J. Physiol. 444, 491–498. https://doi.org/10.1007/s00424-002-0831-z.

Margrie, T.W., Meyer, A.H., Caputi, A., Monyer, H., Hasan, M.T., Schaefer, A.T., Denk, W., Brecht, M., 2003. Targeted whole-cell recordings in the mammalian brain in vivo.

Neuron 39, 911–918. https://doi.org/10.1016/j.neuron.2003.08.012.
Meyer, A.H., Blatow, M., Rozov, A., Monyer, H., Katona, I., 2002. In vivo labeling of parvalbumin-positive interneurons and analysis of electrical coupling in identified neurons. J. Neurosci. 22, 7055–7064 https://doi.org/20026742.
Neher, E., Sakmann, B., 1976. Single-channel currents recorded from membrane of denervated frog muscle fibres. Nature 260, 799–802. https://doi.org/10.1038/260799a0.
Nieweg, K., Andreyeva, A., Van Stegen, B., Tanriöver, G., Gottmann, K., 2015. Alzheimer's disease-related amyloid-β induces synaptotoxicity in human iPS cell-derived neurons. Cell Death Dis. 6https://doi.org/10.1038/cddis.2015.72. e1709.
Okada, Y., 2012. Patch Clamp Techniques from Beginning to Advanced Protocols. Springer, Tokyo/New York. https://doi.org/10.1007/978-4-431-53993-3.
Pak, N., Siegle, J.H., Kinney, J.P., Denman, D.J., Blanche, T.J., Boyden, E.S., 2015. Closed-loop, ultraprecise, automated craniotomies. J. Neurophysiol. 113, 3943–3953. https://doi.org/10.1152/jn.01055.2014.
Pala, A., Petersen, C.C.H.C.H., 2015. In vivo measurement of cell-type-specific synaptic connectivity and synaptic transmission in layer 2/3 mouse barrel cortex. Neuron 85, 68–75. https://doi.org/10.1016/j.neuron.2014.11.025.
Pei, X., Volgushev, M., Vidyasagar, T.R., Creutzfeldt, O.D., 1991. Whole cell recording and conductance measurements in cat visual cortex in-vivo. Neuroreport 2, 485–488. https://doi.org/10.1097/00001756-199108000-00019.
Peng, Y., Mittermaier, F.X., Planert, H., Schneider, U.C., Alle, H., Geiger, J.R., 2019. High-throughput microcircuit analysis of individual human brains through next-generation multineuron patch-clamp. bioRxiv. https://doi.org/10.1101/639328. 639328.
Perin, R., Markram, H., 2013. A computer-assisted multi-electrode patch-clamp system. J. Vis. Exp., e50630. https://doi.org/10.3791/50630.
Piatkevich, K.D., Suk, H.J., Kodandaramaiah, S.B., Yoshida, F., DeGennaro, E.M., Drobizhev, M., Hughes, T.E., Desimone, R., Boyden, E.S., Verkhusha, V.V., 2017. Near-infrared fluorescent proteins engineered from bacterial phytochromes in neuroimaging. Biophys. J. 113, 2299–2309. https://doi.org/10.1016/j.bpj.2017.09.007.
Roome, C.J., Kuhn, B., 2018. Simultaneous dendritic voltage and calcium imaging and somatic recording from Purkinje neurons in awake mice. Nat. Commun. 9, 3388. https://doi.org/10.1038/s41467-018-05900-3.
Sakmann, B., Neher, E., 1984. Patch clamp techniques for studying ionic channels in excitable membranes. Annu. Rev. Physiol. 46, 455–472. https://doi.org/10.1146/annurev.ph.46.030184.002323.
Sánchez, D., Johnson, N., Li, C., Novak, P., Rheinlaender, J., Zhang, Y., Anand, U., Anand, P., Gorelik, J., Frolenkov, G.I., Benham, C., Lab, M., Ostanin, V.P., Schäffer, T.E., Klenerman, D., Korchev, Y.E., 2008. Noncontact measurement of the local mechanical properties of living cells using pressure applied via a pipette. Biophys. J. 95, 3017–3027. https://doi.org/10.1529/biophysj.108.129551.
Sigworth, F.J., Neher, E., 1980. Single Na+channel currents observed in cultured rat muscle cells. Nature 287, 447–449. https://doi.org/10.1038/287447a0.
Singer, A.C., Talei Franzesi, G., Kodandaramaiah, S.B., Flores, F.J., Cohen, J.D., Lee, A.K., Borgers, C., Forest, C.R., Kopell, N.J., Boyden, E.S., 2017. Mesoscale-duration activated states gate spiking in response to fast rises in membrane voltage in the awake brain. J. Neurophysiol. 118, 1270–1291. https://doi.org/10.1152/jn.00116.2017.
Stoy, W.A., Kolb, I., Holst, G., Liew, Y.J., Pala, A., Yang, B., Boyden, E.S., Stanley, G.B., Forest, C.R., 2017. Robotic navigation to sub-cortical neural tissue for intracellular electrophysiology in vivo. J. Neurophysiol. 118, 1141–1150. https://doi.org/10.1152/jn.00117.2017. jn.00117.2017.
Stuart, G.J., Dodt, H.U., Sakmann, B., 1993. Patch-clamp recordings from the soma and dendrites of neurons in brain slices using infrared video microscopy. Pflugers Arch. 423, 511–518. https://doi.org/10.1007/BF00374949.
Suk, H.J., van Welie, I., Kodandaramaiah, S.B., Allen, B., Forest, C.R., Boyden, E.S., 2017. Closed-loop real-time imaging enables fully automated cell-targeted patch-clamp neural recording in vivo. Neuron 1037–1047. https://doi.org/10.1016/j.neuron.2017.08.011. e11.
Svoboda, K., Denk, W., Kleinfeld, D., Tank, D.W., 1997. In vivo dendritic calcium dynamics in neocortical pyramidal neurons. Nature 385, 161–165. https://doi.org/10.1038/385161a0.
Ting, J.T., Daigle, T.L., Chen, Q., Feng, G., 2014. Acute brain slice methods for adult and aging animals: application of targeted patch clamp analysis and optogenetics. Methods Mol. Biol. 1183, 221–242. https://doi.org/10.1007/978-1-4939-1096-0_14.
Piatkevich, K.D., Bensussen, S., Tseng, H., Shroff, S.N., Lopez-Huerta, V.G., Park, D., Jung, E.E., Shemesh, O.A., Straub, C., Gritton, H.J., Romano, M.F., Costa, E., Sabatini, B.L., Fu, Z.F., Boyden, E.S., Han, X., 2019. Population imaging of neural activity in awake behaving mice in multiple brain regions. Biorchiv. https://doi.org/10.1101/616094.
van Welie, I., Roth, A., Ho, S.S.N., Komai, S., Häusser, M., 2016. Conditional spike transmission mediated by electrical coupling ensures millisecond precision-correlated activity among interneurons in vivo. Neuron 90, 810–823. https://doi.org/10.1016/j.neuron.2016.04.013.
Wu, Q., Kolb, I., Callahan, B.M., Su, Z., Stoy, W., Kodandaramaiah, S.B., Neve, R.L., Zeng, H., Boyden, E.S., Forest, C.R., Chubykin, A.A., 2016. Integration of autopatching with automated pipette and cell detection in vitro. J. Neurophysiol. 116, 1564–1578. https://doi.org/10.1152/jn.00386.2016.
Zhang, Z., Russell, L.E., Packer, A.M., Gauld, O.M., Häusser, M., 2018. Closed-loop all-optical interrogation of neural circuits in vivo. Nat. Methods 15, 1037–1040. https://doi.org/10.1038/s41592-018-0183-z.
Zhao, Y., Inayat, S., Dikin, D.A., Singer, J.H., Ruoff, R.S., Troy, J.B., 2008. Patch clamp technique: review of the current state of the art and potential contributions from nanoengineering. Proc. Inst. Mech. Eng. Part N J. Nanoeng. Nanosyst. 222, 1–11. https://doi.org/10.1243/17403499JNN149.